

# Speaker-independent Speech Separation with Deep Attractor Network

Zhuo Chen, Yi Luo, and Nima Mesgarani

**Abstract**—Despite the recent success of deep learning for many speech processing tasks, single-microphone speech separation remains challenging for two main reasons. One reason is the arbitrary order of the target and masker speakers in the mixture (permutation problem), and the second is the unknown number of speakers in the mixture (output dimension problem). We propose a novel deep learning framework for speech separation that addresses both of these important issues. We use a neural network to project the time-frequency representation of the mixture signal into a high-dimensional embedding space. A reference point (attractor) is created in the embedding space to pull together all the time-frequency bins that belong to that speaker. The attractor point for a speaker is formed by finding the centroid of the source in the embedding space which is then used to determine the source assignment. We propose three methods for finding the attractor points for each source, including unsupervised clustering, fixed attractor points, and fixed anchor points in the embedding space that guide the estimation of attractor points. The objective function for the network is standard signal reconstruction error which enables end-to-end operation during both the training and test phases. We evaluate our system on the Wall Street Journal dataset (WSJ0) on two and three speaker mixtures, and report comparable or better performance in comparison with other deep learning methods for speech separation.

**Keywords**—Source separation, multi-talker, deep clustering, attractor network

## I. INTRODUCTION

A listener in real-world situations must often separate a speaker’s voice from a mixture of several sound sources including other speakers and a variety of environmental sounds. Humans can do this with ease, even when listening with only one ear. This effortless task for humans however has proven extremely difficult to model and emulate algorithmically and is a challenge that must be solved in order to achieve robust performance in speech processing tasks. For example, while the performance of automatic speech recognition (ASR) systems today have reached that of the humans in clean condition [1], they are still unable to perform well in noisy and reverberant conditions and lack robustness when interfering noise sources are present. This is even more challenging in tasks where separating all the sources in a mixture is required, such as multi-talker meeting transcription and music separation. When signals from multiple microphones are available, beamforming algorithms can be used to improve the target-to-masker ratio [2], [3]. However, where only one microphone is available, the general audio separation problem is still unresolved.

Prior to the emergence of deep learning, three main categories of algorithms were proposed to solve the speech separation problem: *statistical* methods, *clustering* methods, and *factorization* methods. Statistical methods are most suitable for noise removal, and clustering and factorization methods are most suitable for more general audio separation. In statistical methods [4], [5], [6], the distribution of the speech signal is assumed beforehand and modeled using methods such as complex Gaussian distribution. Noise is assumed to be statistically independent from speech and its characteristics can be estimated from non-speech regions. A maximum likelihood process is then formulated based on the known statistical distributions of speech and noise. In clustering methods, the defining characteristics of the target source are estimated from the observation. For example, the characteristic pitch and signal continuity of speech are used to separate it from the other sources in the mixture. Methods of computational auditory scene analysis (CASA) fall into this category [7]. Factorization model, such as non-negative matrix factorization (NMF) [8], forms a convex optimization process, where the time-frequency (T-F) representation of the mixture is factorized into a combination of sources and activations. The activations learned for each source is then used to reconstruct the corresponding source.

Work in deep learning has moved beyond the algorithms discussed above and has made important progress in audio source separation. Specifically, neural networks have been successfully applied in speech enhancement [6], [9], [10] and music separation [11], [12] with significantly better performance compared with traditional methods. The most commonly used algorithm is the “auto-encoder” (AE) neural network. In a typical AE network, the input is the time-frequency representation of the audio mixture (such as noisy speech), and the output of the network is the estimated spectrogram of clean speech, which formulates the separation as a multi-class regression problem. Variations of AE networks have been proposed for different scenarios and problems [13], [14].

The limitations of the AE approach are evident in complex scenarios such as separating two simultaneous speakers. Two main difficulties arising in this situation are the so-called *permutation problem* and the *output dimension mismatch problem*. The *permutation problem* [15] refers to the arbitrary order of the sounds in the mixture. For example, in separating speakers A and B, both (A,B) and (B,A) are acceptable permutations of the sources. However, training a neural network with more than one target label per sample produces conflicting gradients and thus will not converge, because the correct permutation of the targets for each utterance cannot be determined beforehand. For instance, assigning speaker A to the first target position

---

Zhuo Chen and Yi Luo are co-first authors.

in (A,B) and (A,C) will cause confusion when the mixture consists of (B,C), since they both need to be in the second position for consistency with the previous samples. The second problem is the *output dimension mismatch problem*. Since the number of sources in a mixture can vary, a neural network with a fixed number of output targets does not have the flexibility to separate an arbitrary number of sources.

Two deep learning methods, deep clustering (DPCL) [15] and permutation invariant training (PIT) [16] have been proposed recently to resolve these problems. In deep clustering, a network is trained to generate discriminative embedding for each T-F bin so that the embeddings of the T-F bins that belong to the same source are closer to each other. While DPCL is able to solve both the permutation and output dimension problems to produce the state-of-the-art performance, the main drawback is its inability to perform end-to-end optimization since DPCL minimizes the affinity between the sources in the embedding space, not the target signals. In more recent DPCL work, minimizing the separation error is processed with an unfolding clustering system and an additional network trained stage by stage to ensure convergence [17]. The PIT algorithm solves the permutation problem by pooling over all possible permutations for  $N$  mixing sources ( $N!$  permutations), and using the permutation with the lowest error to update the network. PIT was proposed in [16], and was later shown to have comparable performance to DPCL [15]. However, the PIT approach doesn't resolve the output dimension mismatch problem because it assumes a fixed number of sources.

In this work, we address the general source separation problem with a novel deep learning framework which we refer to as the "attractor network". The term "attractor" refers to the well-studied perceptual effects in human speech perception which suggest that the biological neural networks create perceptual attractors (magnets) that warp the acoustic feature space to attract the sounds that are close to them, a phenomenon that is called the Perceptual Magnet Effect [18]. Our proposed model works on the same principle by forming a reference point (attractor) for each source in the embedding space which draws all the T-F bins belonging to that source toward itself. A mask is estimated for each source in the mixture using the distance measurement between the embeddings and each attractor. Since the correct permutation of the masks is directly related to the permutation of the attractors, our attractor network can potentially be extended to an arbitrary number of sources without the permutation problem once the order of attractors is established. Our framework also enables efficient end-to-end training without the need for additional modules such as the soft-clustering subnetwork [17].

The rest of the paper is organized as follows. In Section II, we briefly review the deep clustering and the permutation invariant training. In Section III, we describe our attractor network and discuss its operation in detail. In Section III-C, we extend our model by combining it with permutation invariant training, which makes it more stable and powerful. In Section V, we evaluate the performance of the attractor network and analyze the properties of the embedding space.

## II. DEEP CLUSTERING AND PERMUTATION INVARIANT TRAINING

### A. Deep clustering

The objective of deep clustering is shown in Eqn. 1

$$\mathcal{L}_{\text{DPCL}} = \|\hat{\mathbf{A}} - \mathbf{A}\|_F^2 = \|\mathbf{V}\mathbf{V}^T - \mathbf{Y}\mathbf{Y}^T\|_F^2 \quad (1)$$

In Eqn. 1, for each T-F bin in a mixture spectrogram, a high-dimensional representation  $V \in \mathbb{R}^{t_f, k}$ , referred to as embedding, is learned by a neural network transformation  $\Phi(\odot)$ , from which the affinity matrix of the sources is formed through  $\hat{\mathbf{A}} = \mathbf{V}\mathbf{V}^T$ . The training objective in this case minimizes the distance between the learned and actual ( $\mathbf{A} = \mathbf{Y}\mathbf{Y}^T$ ) affinity matrices. During the test phase, a clustering algorithm such as K-means is applied to the embedding matrix  $\mathbf{V}$  to generate a cluster assignment matrix.

Since the affinity optimizes in-group and out-group separation, the DPCL does not suffer from the permutation problem discussed in the previous section. Moreover, the number of mixing sources only affects the rank of the affinity matrix  $\mathbf{A} \in \mathbb{R}^{f_t, f_t}$ , while its size remains the same. Therefore DPCL can handle a mixture with a variable number of sources, and the approximate rank of the learned affinity can be used as an important indicator for the number of sources.

Because DPCL's training target is the affinity of sources, it is difficult to perform end-to-end optimization (i.e. directly minimizing the reconstruction error of the clean signals) or combine with other networks (e.g. an speech recognition network). One approach [17] combined DPCL with additional unfolded layers for soft-kmeans clustering together with a second-stage speech enhancement network.

### B. Permutation invariant training

In permutation invariant training, the network estimates a mask for each source and directly minimizes the distance between reconstruction and the clean target. The permutation problem between the network output and the label is solved by pooling through all permutations (i.e. measuring the training error of all permutations and pick the one with minimum error). While the PIT approach can perform end-to-end optimization, the output dimension is fixed, leading to difficulties when dealing with an unknown number of sources in the mixture.

## III. DEEP ATTRACTOR NETWORK

Our Deep Attractor Network (DANet) model can be efficiently implemented as an end-to-end system because it directly minimizes the reconstruction error of the sources (as opposed to maximizing separation), and is able to deal with a variable number of sources in a mixture.

### A. Formulation of the model

The first stage of the DANet system is a neural network trained to map the mixture sound  $X$  to a  $K$ -dimensional embedding space, such that to minimize the following objective function

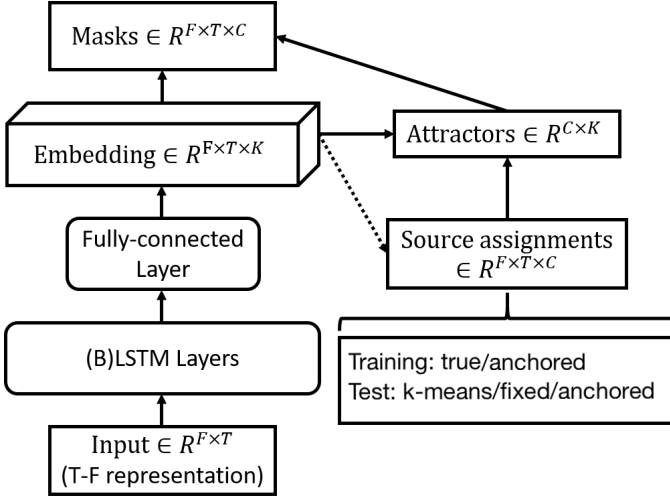


Fig. 1. The system architecture. The signal is projected into a high-dimensional embedding space where the projected time-frequency bins of each source are pulled toward several attractor points in the embedding space. During the training phase, the attractors are formed using true or estimated (in anchored DANet) source assignments. During the test phase, the attractors are formed in three alternative ways using: unsupervised clustering, fixed points, or fixed anchor points.

$$\mathcal{L} = \sum_{f,t,c} \|S_{f,t,c} - X_{f,t} \times M_{f,t,c}\|_2^2 \quad (2)$$

where  $S$  is the clean spectrogram (frequency  $F \times$  time  $T$ ) of  $C$  sources,  $X$  is the mixture spectrogram (frequency  $F \times$  time  $T$ ), and  $M$  is the mask formed to extract each source. The mask is estimated in the  $K$ -dimensional embedding space of each T-F bin, represented by  $V \in \mathbb{R}^{F \times T \times K}$

$$D_{c,f,t} = \sum_k A_{c,k} \times V_{f,t,k} \quad (3)$$

$$M_{c,f,t} = \mathcal{H}(D_{c,f,t}) \quad (4)$$

where  $D$  is the distance between embeddings and each attractor point,  $\mathcal{H}$  is the nonlinearity function for generating the masks, which can be either a sigmoid or softmax function, and  $A \in \mathbb{R}^{C \times K}$  are the attractor points for the  $C$  sources in the embedding space, learned during training, defined as

$$A_{c,k} = \frac{\sum_{f,t} V_{k,f,t} \times Y_{c,f,t}}{\sum_{f,t} Y_{c,f,t}} \quad (5)$$

where  $Y \in \mathbb{R}^{F \times T \times K}$  is the source assignment function for each T-F bin, meaning that  $Y_{t,f,c} = 1$  if source  $c$  has the highest energy at time  $t$  and frequency  $f$  compare to the other sources.

Next, we estimate a reconstruction mask for each source by finding the similarity of each T-F bin in the embedding space to the attractor points  $A$ , whose similarity is defined in Eqn. 4. This particular measure uses the inner product followed by a nonlinearity function which scales the masks to  $[0, 1]$ . Intuitively, the closer an embedding of a T-F bin is to an attractor, the more likely that T-F bin belongs to the source corresponding to that attractor, and therefore the resulting mask for that source will produce larger values for that T-F bin.

Finally, a standard  $L^2$  reconstruction error is used to generate the gradient, as shown in Eqn. 2. The error for each source reflects the difference between the masked signal and the clean reference, forcing the network to optimize the global reconstruction error for better separation by changing both the embedding and the location of attractor points. In our model, the attractor points behave as magnets in the embedding space that pull all the points that belong to the same source. Thus we refer to the proposed model as a deep attractor network (DANet).

### B. Relation to DPCL and PIT

DANet has several advantages and appealing properties when compared to previous methods. Compared with the deep clustering, DANet performs end-to-end optimization using a significantly simpler model. In addition, direct reconstruction of each source in DANet allows the system to easily integrate with other tasks such as speech recognition, or combine with different optimizing criteria such as phase-aware distance [19] or KL-divergence.

On the other hand, when the attractor points are considered as a layer in the network instead of dynamically formed by the embeddings, DANet reduces to a classification network [9], [6], and Eqn. 2 becomes a fully-connected layer. In this case, permutation invariant training becomes necessary since the mask is not directly linked to a source. In contrast with PIT which directly models the entire separation process, DANet has the advantage and flexibility of forming attractor points during the training. This allows the system to use the affinity between the samples without constraining the number of patterns that can be found, therefore allowing the network to deal with a variable number of sources in the mixture. In addition, DANet's formation of attractor points in the embedding space allows for incorporating source dependent knowledge such as the mixing source or potentially speaker-specific attractor points.

### C. Estimation of attractor points

In addition to the simple averaging over the embeddings of a source shown in Eqn. 5, attractor points can be estimated using a number of methods to allow more stable estimation and faster processing. One possibility is to use a weighted average instead, where the the embedding of T-F bins with smaller power are weighted less. Since the attractor points represent the center of gravity of each source, averaging over the embedding points that correspond to the most salient T-F bins (i.e. the T-F bins where the source has higher power) leads to more robust estimation of attractor points. We investigated this strategy using a threshold on the mixture magnitude spectrogram of the T-F bins included in the estimation of the attractor. A neural network model may also be used to pick the representative embedding for each source, an idea which shares similarities with encoder-decoder attention networks [20], [21].

## IV. ALTERNATIVE METHODS TO FORM ATTRACTOR POINTS

As described in 5, the true source assignment of the embeddings  $Y$  is necessary to form the attractor points during

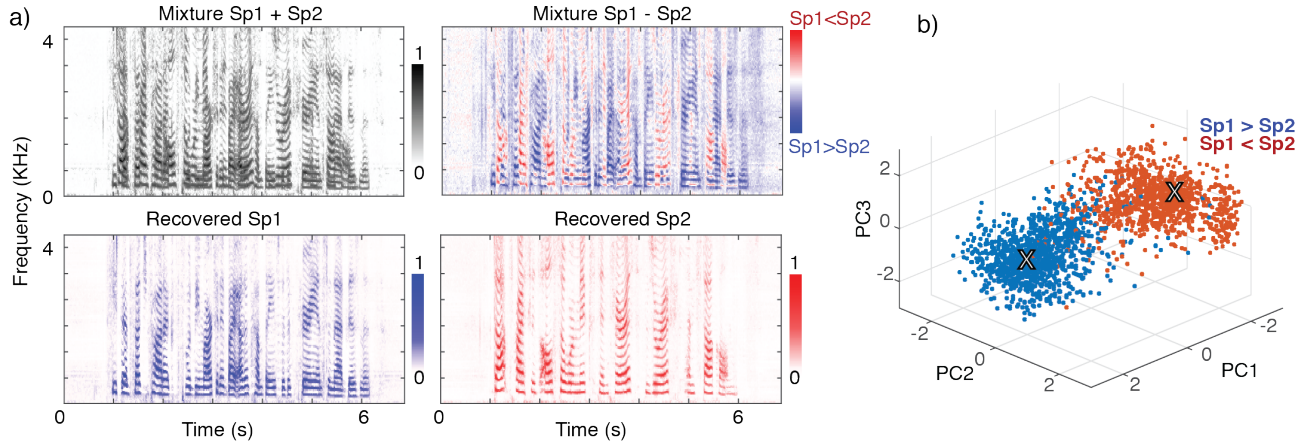


Fig. 2. a) an example of the mixture spectrogram and the recovered speakers. b) Location of T-F bins in embedding space. Each dot visualizes the first three principle components of the embedding of one T-F bin, where colors distinguish the relative power of speakers in that bin. The location of the attractor points is marked with X.

the training phase of DANet. However, this information is not available during the test phase. In this section, we propose several methods to approximate the position of the attractor points during the test phase and discuss their cons and pros.

The simplest method is to use an unsupervised clustering algorithm such as K-means [15] to determine the source assignment. This process has several limitations. First, the K-means step increases the computational cost of the system and therefore increases the run time delay. More importantly, the center from K-means step is not guaranteed to match the true location of the attractor points. This potential departure of the attractor points during the test phase from the actual assignment, as shown in Eqn. 5, causes a mismatch in the mask formation between the training and test phases.

One such example is shown in Fig. 3, where the embedding space is visualized using its first two principle components. The location of actual and estimated attractor points is plotted in yellow and black, and the distance between the two shows the mismatch between the actual and estimated location of attractor points. As suggested by Eqn. 4, this mismatch changes the mask estimated for each source and thus reduces the accuracy of the separation. We refer to this problem as the *center mismatch problem*.

To remedy this problem, we propose two methods for forming the attractor points: 1) fixing the position of attractor points, and 2) fixing reference points in the embedding space (anchor points) that can be used to estimate attractors for each mixture.

#### A. Fixed attractor points

While there is no direct constraint for the location of the attractor points in the embedding space, we have shown empirically that the location of the attractor points is relatively constant across different mixtures. Fig. 5 shows the location of attractors for 10000 different mixture sounds, with each opposite pair of dots corresponding to the attractor points for the two speakers in a given mixture. Two pairs of attractor points (marked as A1 and A2) are automatically discovered by

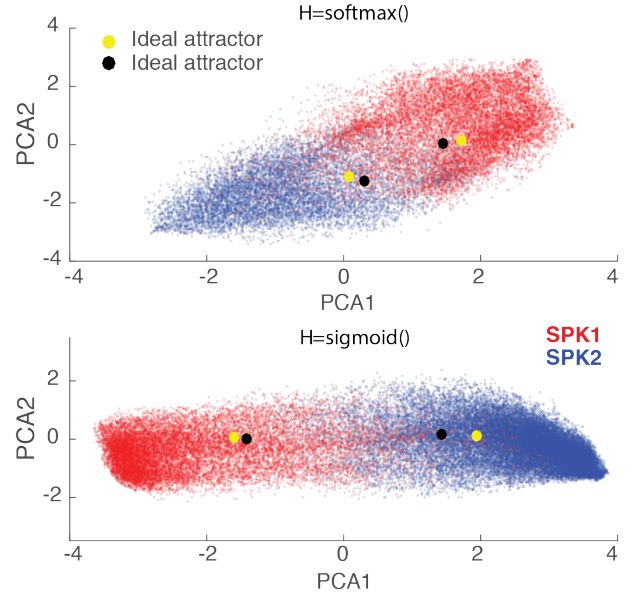


Fig. 3. The gap between the true location of attractors (yellow dots) and the location estimated using K-means clustering (black dots) in the embedding space, in two networks with softmax and sigmoid nonlinearities for mask generation. Blue and red dots show the PCA projection of the embedding of T-F bins corresponding to speakers one and two.

DANet network. This result is likely related to the complexity of the mixture and needs to be further investigated when the signal condition changes.

Based on this observation, we propose to first estimate the attractor points in the training phase, and subsequently fix their locations and use them during the test phase. The advantage of using fixed attractor points is that it removes the need for the unsupervised clustering of the embeddings, allowing the system to directly estimate the mask for each time frame which enables real-time implementation. However it relies on the assumption that the location of the attractor points in training

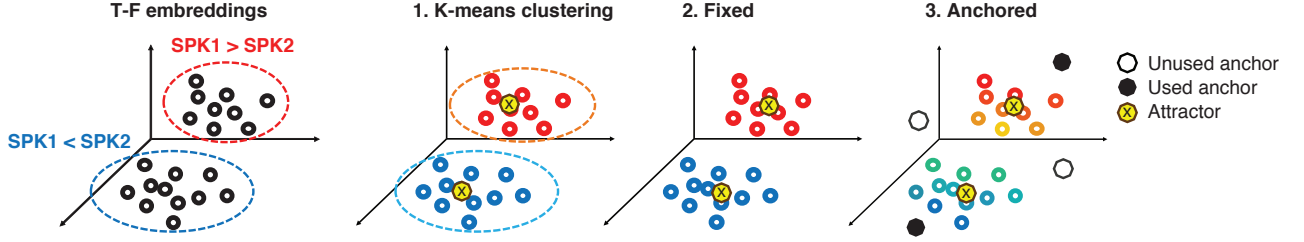


Fig. 4. An illustration of different ways for attractor calculation in DANet. If the true assignment is used during training phase, in test phase either K-means clustering or fixed attractors calculated from training set can be used for estimating the attractors. If anchor points are used for calculating the source assignment, then the test phase processing is the same as the training phase, which leads to a completely end-to-end system.

and test phases are similar, which may not hold if the test condition is significantly different from the training.

### B. Anchored attractor points

A potential problem of both clustering and fixed attractor method is the possible mismatch between the location of attractor points during the training and test phase. This mismatch may be problematic when the signal condition changes drastically between the two, as the fixed attractor points found in the training may be different from the true attractor of the test utterances. In addition, clustering is not guaranteed to work in cases where the embedding of the sources may not be separated enough. The reason for the center mismatch problem is the unknown source assignment of the T-F bins during the test phase, which is the information that is used to form the attractor points during the training phase. To remove the center mismatch problem, a similar method needs to be used during both the training phase and the test phase. In other words, the true source assignment should also not be explicitly used during the training.

To address these problems, we propose a generalized Expectation-Maximization (EM) framework where the separation is processed through a one step “expectation” and “maximization” iteration. This extended framework separates the sources in the mixture in four steps:

First, the matrix  $V$  is generated by projecting the T-F bins to a high-dimensional embedding space, similar to the generation of embedding points using DANet.

Second, an “E-step” is applied for calculating source assignment by creating several randomly initialized points in the embedding space, which we refer to as the *anchor points*. The distance between the embedding and the anchor points is used to estimate the source assignment for each embedding. More specifically, let  $I \in \mathbb{R}^{N \times K}$  be  $N$  anchors, then for each anchor set  $H_p \in \mathbb{R}^{C \times K}$  in all  $C$ -combination of the fix anchors,  $C$  weight matrices are calculated by

$$W_{p,c,ft} = \text{Softmax}(\sum_k H_{p,c,k} \times V_{ft,k}) \quad (6)$$

where  $P = \binom{N}{C}$  is the total number of  $C$ -combinations, and  $p = 1, 2, \dots, P$  is the index of anchor sets. The softmax function is used to increase the contrast between the weights.

Third, given the source assignments estimated from the anchor points, an “M-step” is used to estimate the attractor locations using the same procedure as the standard DANet in Eqn. 5, where the location of the attractor points is calculated based on the assignments given by the anchor point set  $H_p$ , using the weighted average of the embeddings.

$$A_{p,c,k} = \frac{\sum_{f,t} V_{k,ft} \times W_{p,c,ft}}{\sum_{f,t} W_{p,c,ft}} \quad (7)$$

Since only one attractor (mask) can be used for estimating the mask for a given source, we choose the set of attractor points based on the in-set similarity of the attractor sets. The in-set similarity is defined as the maximum similarity of any of the two attractors within the attractor set

$$S_p = \max_k \{ \sum_k A_{p,i,k} \times A_{p,j,k} \}, \quad 1 \leq i < j \leq C \quad (8)$$

Note that for the consistency, we use dot product to measure the similarity, resulting in larger values denoting smaller distances.

Finally, we select the attractor set with the smallest in-set similarity (i.e. largest distance)

$$\hat{A} = \argmin \{ S_p \}, \quad 1 \leq p \leq P \quad (9)$$

and then use it to estimate the mask for each source in the same way as the original DANet in Eqn. 4. Note that during the training phase, the location of the anchor points is adaptively learned jointly with the embeddings, and is subsequently fixed during the test phase. Algorithm 1 shows the entire process of this network.

Fig. 6 shows examples of the position of the embeddings and the anchor points in a 6-anchor point network for two different mixture conditions (2 and 3 speaker mixture).

Compared with the clustering based approach or fixed attractor approach, the fixed anchor point approach eliminates the need for true source assignment of T-F bins during both training and test phases. The center mismatch problem no longer exists because the attractor points are determined by the anchor points, which is deterministic for a given mixture. The mask generation process is therefore fully end-to-end during both training and test phases.

The two drawbacks of the anchor point approach are that the correct permutation of the anchor points is unknown, therefore



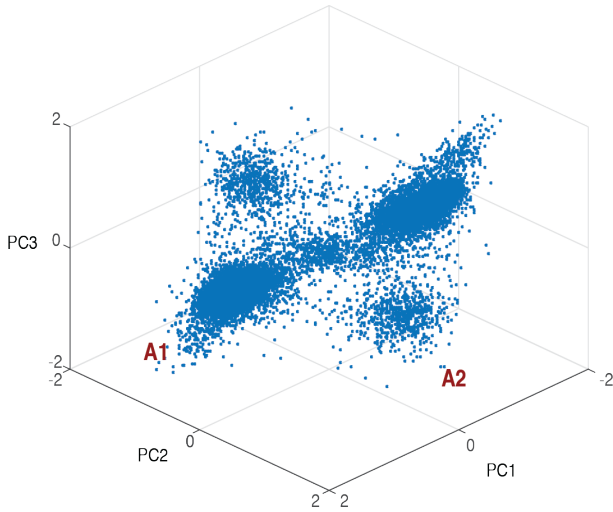


Fig. 5. Location of attractor points in the embedding space in a sigmoid network. Each dot corresponds to one of the 10000 mixtures sounds, visualized using the first three principal components. Two distinct attractor pairs are visible (denoted by A1 and A2).

---

**Algorithm 1** DANet with fixed anchor points for attractor formation

---

**Input:** mixture spectrogram  $X$ , adaptable anchor points  $H_p$ , number of speaker  $C$

**Output:** Estimated masks  $M_e$

- 1: **Initialization:** Randomly initialize  $H_p$
  - 2: **for** Each batch in training set **do**
  - 3:   Produce embeddings of T-F bins:  $V_{k,ft}$
  - 4:   **E step:** Calculate source assignment matrix  $W_{p,c,ft}$  for all  $C$ -combination of anchor point in  $H_p$
  - 5:   **M step:** Estimate attractors  $A_{p,c,k}$  using  $W_{p,c,ft}$ , choose the attractors with maximum separation
  - 6:   Estimate masks  $M_e$  using  $\hat{A}_{c,k}$  and  $V_{k,ft}$
  - 7:   Back-propagate gradients
  - 8: **end for**
- 

PIT is required during the training phase. Also, since  $P = \binom{N}{C}$  combinations of EM iterations is required for attractor generation and selection, the computational complexity is higher when the number of anchor points  $N$  is large.

## V. EXPERIMENT AND ANALYSIS

We evaluate our proposed model on the task of single-channel two and three speaker separation. Example sounds can be found here [22].

### A. Data

We use the WSJ0-2mix and WSJ0-3mix datasets introduced in [15] which contains two 30 h training sets and a 10 h validation sets for the two tasks generated by randomly selecting utterances from different speakers in the Wall Street Journal (WSJ0) training set si\_tr\_s, and mixing them at various signal-to-noise ratios (SNR) randomly chosen between 0 dB

and 5 dB. Two 5 h evaluation sets are generated in the same way, using utterances from 16 unseen speakers from si\_dt\_05 and si\_et\_05 in the WSJ0 dataset. All data are resampled to 8 kHz to reduce computational and memory costs. The log spectral magnitude serves as the input feature, computed using short-time Fourier transform (STFT) with 32 ms window length, 8 ms hop size, and the square root of hanning window.

We evaluated the separation performance using signal-to-distortion ratio (SDR), which we define as scale-invariant signal-to-noise ratio (SNR) [17].

### B. Network architecture

The network contains 4 Bi-directional LSTM [23] layers with 600 hidden units in each layer. The embedding dimension is set to 20, resulting in a fully-connected feed-forward layer of 2580 hidden units ( $20 \times 129$ ) after the BLSTM layers. We split the input features into non-overlapping chunks of 100-frame length as the input to the network. Adam algorithm [24] is used for training, with the learning rate starting at  $3e^{-4}$  and then halved if no best validation model is found in 3 epochs. The total number of epochs is set to 100, and we used the cost function in Eqn. 2 on the validation set for early stopping. The criteria for early stopping is no decrease in the loss function on validation set for 10 epochs. No further regularization is applied in the models. The wiener-filter like mask [13] is used as the training target.

During training, we split the input into 100-frame long segments, and then continue training the network with 400-frame long segments, which is known as the curriculum training strategy [25].

### C. Results

Table I shows the results of different magnitude threshold used for attractor formation, as well as the effect of the nonlinearity functions for mask generation. Sigmoid networks tend to have more stable performance when K-means clustering is used compared with the true location of attractor points, while softmax may lead to a larger gap between K-means and true attractor positions. This can be explained by the property of sigmoid and softmax. Unlike softmax, sigmoid does not have the explicit constraint that the summation of the masks should add up to one. For T-F bins where the target mask is very close to 0 or 1 (i.e. one speaker is significantly stronger or weaker than the other), the input to the sigmoid function should be large enough or small enough to match the target. This requirement pushes the embeddings toward or away from the attractors. Fig. 7 visualizes the gap between the distances of embeddings from different attractor points, i.e.,  $D_0 - D_1$  in a two-speaker separation task. This implicitly ensures that the embeddings are separated enough for K-means to estimate the attractors. Softmax, however, is less sensitive to the absolute distance between embeddings and the attractors, since the  $e^x$  term in softmax grows or vanishes rapidly as the input  $x$  increases or decreases. Since the range of input  $x$  to softmax is  $[-N, N]$ , when input dimension  $N$  is large, little difference is observed between  $\frac{e^{-N}}{e^{-N} + e^N}$  and

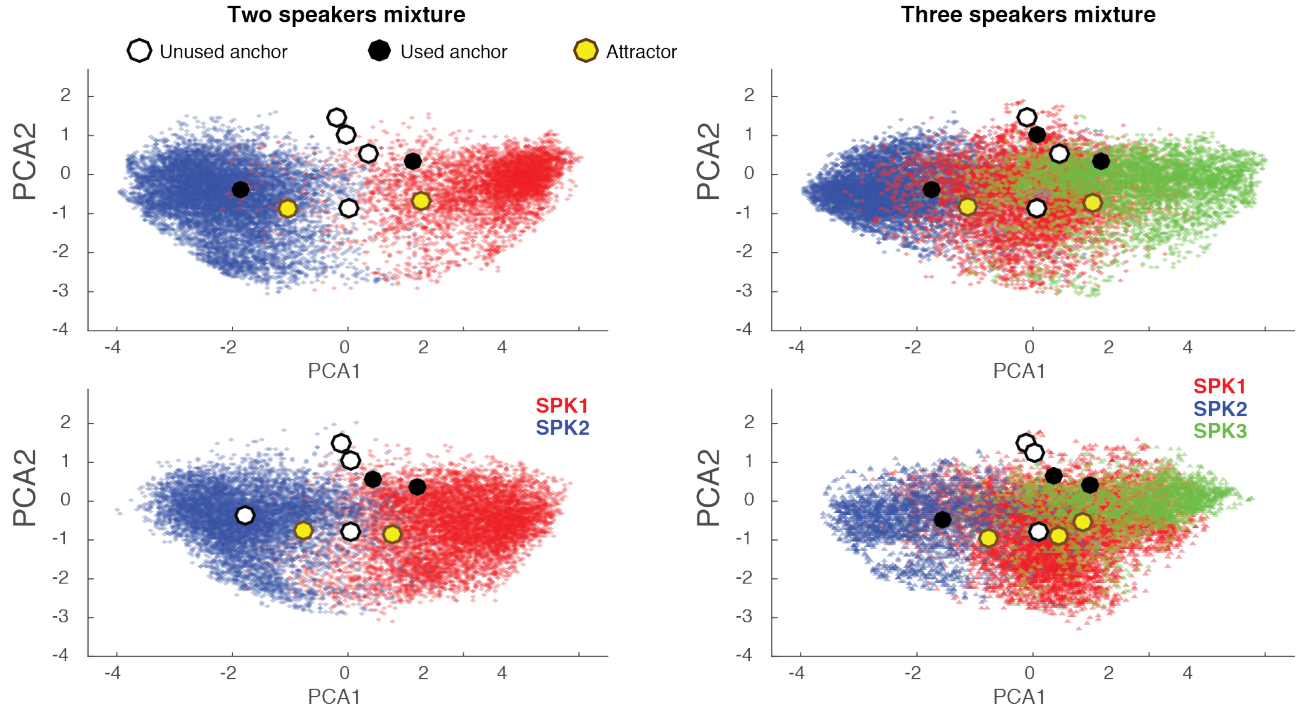


Fig. 6. The PCA projection of the embeddings of the speakers (SPK1..3), anchor points, and attractor points (yellow) for two different mixtures in a 6-anchor point DANet. As can be seen, different anchor points are selected for different mixtures, proving more flexibility and stability in different conditions.

$\frac{e^0}{e^0 + e^N}$ . While the embeddings for some T-F bins are very different from each other, similar mask values can be observed, making it difficult for K-means to accurately estimate the position of the ideal attractors (Fig. 3). Hence, although the softmax network has higher ideal performance, the K-means performance is not as good with sigmoid. Our results also show that the K-means performance of the softmax network is highly dependent on how the network is optimized, i.e., different network trained with different initializations may have very different performance, with a similar level of validation error. This observation is supported by our assumption that softmax is less sensitive to the distance when the embedding dimension is high. Adding a training regularization such as dropout does not guarantee improved performance.

TABLE I. SDR IMPROVEMENT (SDRi) IN DECIBEL ON WSJ0-2MIX WHERE ALL, OR TOP 90% EMBEDDING POINTS ARE USED TO FORM ATTRACTORS.  
\* DENOTES CURRICULUM TRAINING.  
(-FIXED: USING FIX ATTRACTORS CALCULATED FROM TRAINING SET)

	$\mathcal{H}$	K-means	ideal
DANet-all	Sigmoid	9.3	9.6
DANet-90%	Sigmoid	9.5	9.7
DANet-90%-fixed	Sigmoid	9.2	-
DANet-90%*	Sigmoid	<b>10.3</b>	10.6
DANet-90%	Softmax	9.4	9.9
DANet-90%*	Softmax	10.0	10.8

Table II shows the effect of changing the number of anchor

points in a network with softmax function used for mask generation. As the number of anchor points increases, the performance of the network constantly improves. It confirms that the increased flexibility in the choice of the anchor points help the final separation performance. Unlike softmax DANet with K-means, adding dropout in BLSTM layers here is guaranteed to increase the performance. This shows the advantage of the end-to-end framework without the unstable clustering step.

TABLE II. SDR IMPROVEMENT (SDRi) ON THE WSJ0-2MIX WITH VARYING NUMBERS OF ANCHOR POINTS.  
\* DENOTES CURRICULUM TRAINING.

# of anchor points	dropout rate	SDRi (dB)
2	0	9.3
2	0.5	9.4
4	0	9.5
4	0.5	9.8
6	0	9.6
6	0.5	9.8
6*	0	10.1
6*	0.5	<b>10.4</b>

Table III compares our system with other systems with different configurations. Note that PIT-T-BLSTM-ST and DPCL++ in this table are two-stage systems (where a second neural network is used to optimize the estimated mask) and all other systems perform separation in one step. Our K-means DANet system outperforms all the one-stage systems, and has comparable results as the two-stage PIT-T-BSTLM-ST system

which uses dropout during training [26]. Moreover, our anchor point DANet outperforms all systems except for DPCL++, which is a two-stage method and has many more parameters compared with our system.

Because of the importance of real-time implementation, we also investigated the efficacy of a DANet using LSTM instead of BLSTM for the recurrent layers. We can see from the results that the LSTM-DANet significantly outperforms PIT-LSTM.

TABLE III. COMPARISON OF DANET WITH OTHER METHODS ON WSJ0-2MIX.

Method	SDRi (dB)
DPCL	5.8
PIT-T-BLSTM	9.4
PIT-T-BLSTM-ST	10.0
DPCL++	<b>10.8</b>
DANet-Kmeans*	10.0
DANet-fixed*	9.9
DANet-6 anchor*	<b>10.4</b>
PIT-T-LSTM	7.0
DANet-Kmeans-LSTM*	8.6
DANet-6 anchor-LSTM*	<b>9.0</b>

Table IV shows the performance on the WSJ0-3mix test set. In this three speaker separation task, K-means performs very well on estimating the attractors, possibly because the additional speaker forces the embeddings of different speakers to be more separated in order to recover three masks accurately during training. The fixed anchor point DANet has comparable performance with K-means DANet, however adding the number of anchor points does not improve the performance, presumably because of a smaller mismatch between ideal attractors and the attractors estimated by K-means.

Table V shows the results in the speaker separation task where the same network is used to separate 2 and 3 speaker mixtures. The networks is first trained on three speaker mixtures, and after convergence, we continue the training using both two speaker and three speaker mixtures. K-means DANet performs well on the three speaker separation task, but has worse performance on two-speaker separation. However, the fixed anchor point DANet performs well on both conditions. As we already shown in Fig. 6, different anchor points are chosen for different mixtures, which exemplifies the flexibility of the fixed anchor point network in dealing with various speaker mixtures.

TABLE IV. COMPARISON OF ATTRACTOR ESTIMATION METHODS ON WSJ0-3MIX. (-DO: .5 DROPOUT).

\* DENOTES CURRICULUM TRAINING.

Type	# of anchor points	SDRi (dB)
DANet-Kmeans	-	8.0
DANet-Kmeans*	-	8.6
DANet-anchor	3	8.1
DANet-anchor	4	8.1
DANet-anchor	6	8.1
DANet-anchor*	6	8.5
DANet-anchor-do*	6	<b>9.1</b>

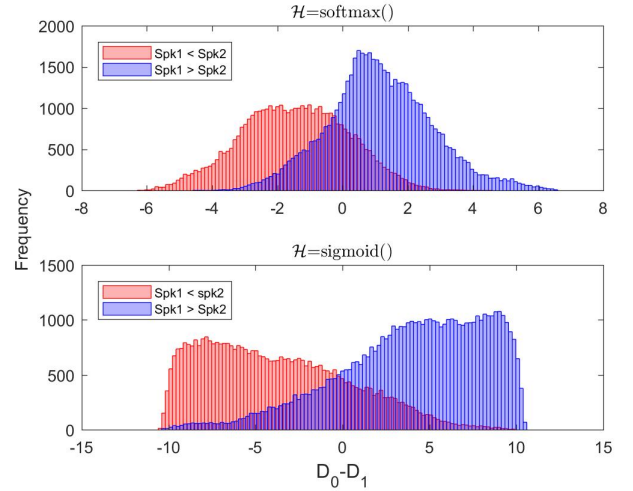


Fig. 7. Histograms of the gap between the distance between the embeddings and the two attractors, i.e.,  $D_0 - D_1$ .

TABLE V. SDR IMPROVEMENTS FOR 2 AND 3 SPEAKER MIXTURES TRAINED ON BOTH WSJ0-2MIX AND WSJ0-3MIX.

Type	2 Spk	3 Spk
DANet-Kmeans*	9.9	5.0
DANet-6 anchor*	<b>10.1</b>	<b>7.5</b>

## VI. CONCLUSION

Our novel deep learning method, deep attractor network (DANet), is proposed for single-microphone speech separation. DANet extends the deep clustering framework by creating attractor points in the embedding space which pull together the embeddings that belong to a specific source, where each attractor point is used to form a separation mask for each source in the mixture. Directly maximizing the reconstruction accuracy allows for end-to-end training. We explored unsupervised clustering of embeddings, fixed attractor points, and fixed anchor points for the estimation of the attractor points. The fixed anchor points approach provides the most flexible solution along with Expectation-Maximization strategy used to deterministically locating the attractor points from the source assignment, which is found from the distance of the embeddings to the anchor points. This approach maintains the utterance-level flexibility of attractor formation, and can generalize better to changing signal conditions. The concept of applying EM style clustering is similar to [17], where an unfolded soft K-means clustering was incorporated in the training. In contrast, the cluster parameters (i.e. assignment and attractors) of our model can vary from one mixture to the next, since they are jointly determined by the anchor points and the current embedding. This utterance-dependent estimation of the attractor points therefore allows for a more flexible method for choosing the best separation mask. Compared with the PIT, the advantage of fixed anchor points is that the number of outputs (clusters) is only limited by the number of anchor points used. Therefore, a network with sufficient number of anchor points can be used to separate an arbitrary number of sources, as we



have shown for two and three speakers in this paper.

DANet is a full end-to-end system for both the training and test phases. Our evaluation shows that DANet has comparable or better performance than previous deep learning frameworks in both causal and non-causal implementations, and also enables the ability to separate varying number of speakers in the mixture with only one network.

## VII. ACKNOWLEDGEMENT

The authors would like to thank Drs. John Hershey and Jonathan Le Roux of Mitsubishi Electric Research Lab, and Dr. Dong Yu of Microsoft Research for constructive discussions. Zhuo Chen and Yi Luo contributed equally to this work. This work was funded by a grant from National Institute of Health, NIDCD, DC014279, National Science Foundation CAREER Award, and the Pew Charitable Trusts.

## REFERENCES

- [1] W. Xiong, J. Droppo, X. Huang, F. Seide, M. Seltzer, A. Stolcke, D. Yu, and G. Zweig, "Sachieving human parity in conversational speech recognition," *arXiv preprint arXiv:1610.05256*, 2016.
- [2] Y. Cao, S. Sridharan, and A. Moody, "Multichannel speech separation by eigendecomposition and its application to co-talker interference removal," *IEEE Trans. on Audio, Speech and Language Processing*, vol. 5, no. 3, 1997.
- [3] R. M. Toroghi, F. Faubel, and D. Klakow, "Multi-channel speech separation with soft time-frequency masking," in *Interspeech 2012*, 2012.
- [4] S. Arberet, A. Ozerov, R. Gribonval, and F. Bimbot, "Blind spectral-gmm estimation for underdetermined instantaneous audio source separation," in *International Conference on Independent Component Analysis and Signal Separation*, 2009, pp. 751–758.
- [5] E. Vincent, M. Jafari, S. Abdallah, M. Plumbley, and M. Davies, "Probabilistic modeling paradigms for audio source separation," *Machine Audition: Principles, Algorithms and Systems*, 2010.
- [6] X. Lu, Y. Tsao, S. Matsuda, and C. Hori, "Speech enhancement based on deep denoising autoencoder," in *Interspeech 2013*, 2013, pp. 436–440.
- [7] D. Wang and G. J. Brown, *Computational auditory scene analysis: Principles, algorithms, and applications*. Wiley-IEEE Press, 2006.
- [8] D. D. Lee and H. S. Seung, "Algorithms for non-negative matrix factorization," in *Advances in neural information processing systems*, 2001, pp. 556–562.
- [9] Z. Chen, S. Watanabe, H. Erdoğan, and J. R. Hershey, "Speech enhancement and recognition using multi-task learning of long short-term memory recurrent neural networks," in *Interspeech 2015*. ISCA, 2015, pp. 3274–3278.
- [10] T. Hori, Z. Chen, H. Erdogan, J. R. Hershey, J. Le Roux, V. Mitra, and S. Watanabe, "The merl/sri system for the 3rd chime challenge using beamforming, robust feature extraction, and advanced speech recognition," in *2015 IEEE Workshop on Automatic Speech Recognition and Understanding (ASRU)*. IEEE, 2015, pp. 475–481.
- [11] P.-S. Huang, M. Kim, M. Hasegawa-Johnson, and P. Smaragdis, "Singing-voice separation from monaural recordings using deep recurrent neural networks," *ISMIR 2014*, 2014.
- [12] Y. Luo, Z. Chen, J. L. Roux, J. R. Hershey, and N. Mesgarani, "Deep clustering and conventional networks for music separation: Stronger together," in *2017 IEEE International Conference on Acoustics, Speech and Signal Processing (ICASSP)*. IEEE, 2017.
- [13] H. Erdogan, J. R. Hershey, S. Watanabe, and J. Le Roux, "Phase-sensitive and recognition-boosted speech separation using deep recurrent neural networks," in *2015 IEEE International Conference on Acoustics, Speech and Signal Processing (ICASSP)*. IEEE, 2015, pp. 708–712.
- [14] F. Weninger, J. Le Roux, J. Hershey, and B. Schuller, "Discriminatively trained recurrent neural networks for single-channel speech separation," in *Signal and Information Processing (GlobalSIP), 2014 IEEE Global Conference on*. IEEE, 2014, pp. 577–581.
- [15] J. R. Hershey, Z. Chen, J. Le Roux, and S. Watanabe, "Deep clustering: Discriminative embeddings for segmentation and separation," in *2016 IEEE International Conference on Acoustics, Speech and Signal Processing (ICASSP)*. IEEE, 2016, pp. 31–35.
- [16] D. Yu, M. Kolbæk, Z.-H. Tan, and J. Jensen, "Permutation invariant training of deep models for speaker-independent multi-talker speech separation," *arXiv preprint arXiv:1607.00325*, 2016.
- [17] Y. Isik, J. L. Roux, Z. Chen, S. Watanabe, and J. R. Hershey, "Single-channel multi-speaker separation using deep clustering," *arXiv preprint arXiv:1607.02173*, 2016.
- [18] P. K. Kuhl, "Human adults and human infants show a perceptual magnet effect for the prototypes of speech categories, monkeys do not," *Attention, Perception, & Psychophysics*, vol. 50, no. 2, pp. 93–107, 1991.

- [19] A. Gaich and M. Pejman, "On speech quality estimation of phase-aware single-channel speech enhancement," in *2015 IEEE International Conference on Acoustics, Speech and Signal Processing (ICASSP)*. IEEE, 2015, pp. 216–220.
- [20] D. Bahdanau, K. Cho, and Y. Bengio, "Neural machine translation by jointly learning to align and translate," *arXiv preprint arXiv:1409.0473*, 2014.
- [21] K. Cho, A. Courville, and Y. Bengio, "Describing multimedia content using attention-based encoder-decoder networks," *IEEE Transactions on Multimedia*, vol. 17, no. 11, pp. 1875–1886, 2015.
- [22] [naplab.ee.columbia.edu/danet](http://naplab.ee.columbia.edu/danet).
- [23] S. Hochreiter and J. Schmidhuber, "Long short-term memory," *Neural computation*, vol. 9, no. 8, pp. 1735–1780, 1997.
- [24] D. Kingma and J. Ba, "Adam: A method for stochastic optimization," *arXiv preprint arXiv:1412.6980*, 2014.
- [25] Y. Bengio, J. Louradour, R. Collobert, and J. Weston, "Curriculum learning," in *Proc. ICML*, 2009, pp. 41–48.
- [26] N. Srivastava, G. E. Hinton, A. Krizhevsky, I. Sutskever, and R. Salakhutdinov, "Dropout: a simple way to prevent neural networks from overfitting," *Journal of Machine Learning Research*, vol. 15, no. 1, pp. 1929–1958, 2014.